The 2013 World Congress on
Advances in Nano, Biomechanics, Robotics, and Energy Research (ANBRE13)
Seoul, Korea, August 25-28, 2013

Synthesis and Characterization of Sol-gel Deposited Aluminum Oxide at Low Temperatures

Farzana Majid[1)], *Saira Riaz[2)], Talha Ijaz[3)], Muhammad Farooq[4)] and Shahzad Naseem[5)]

[1), 2), 3), 4), 5)] *Centre of Excellence in Solid State Physics*, *University of the Punjab*, *Pakistan*
[2)] saira_cssp@yahoo.com

ABSTRACT

Al_2O_3 is the most versatile material having applications in electronic devices and in lasers. It is stable at high temperatures and chemically inert. Sol-gel method is used to synthesize Aluminum oxide nanoparticles and thin films. Thin films are prepared on glass substrates using spin coater. Surface morphologies are observed by using Hitachi S-3400N SEM. Grain size in the range of ~60-90 nm is observed after centrifugation. Grain size is observed to be strongly dependent on the choice of precursors, synthesis conditions and aging temperature. Optical properties are observed by using J.A. Woolam M-2000 Spectroscopic Ellipsometer. Energy band gap value found to be ~4.13 eV. The refractive index observed in the range of 1.55 to 1.79. Extinction coefficient value observed was ~0.103. Value of real part of dielectric constant found to be ~2.83 and imaginary part ~0.5. These alumina films are also optimized as radiation resistant.

1. INTRODUCTION

Spacecraft, during their orbital life, experiences multiple and extreme environmental conditions. These environmental conditions may be due to natural factors (Vacuum, ionizing radiations, charge particle fluxes, micrometeoroids, atomic oxygen in low earth orbit) and artificial factors (space debris, contaminations, etc) (Tonon 2001). These factors not only influence the mechanical, thermo optical properties for spacecraft but also its performance and life expectancy (Fayazbakhsh 2010). The biggest threat to spacecraft performance and life are the temperature anomalies during its orbital mission. Due to alternating passages of spacecraft in the earth shadow and in front of sun, a spacecraft experiences thermal cycling in the space vacuum (Goueffeon 2009, Yo 2011). This thermal cycling in spacecraft, orbiting the earth, produces thermal stresses inside the vehicle (Sharma1997) and causes a temperature variations in the range of -1400°C and +1400°C (Goueffeon 2011). In the space vacuum, the heat exchange between the spacecraft and its environment is through radiations (Kumar

[1), 3), 4)] Graduate Student
[2), 5)] Professor

1997). The temperature maintenance of spacecraft is managed through radiative exchange between the earth, the moon, deep cold space, the sun and the external parts of spacecraft (Goueffeon 2009). For optimum performance of spacecraft and to get fullest efficiency of its parts, the thermal system of the spacecraft must be designed carefully (Qin 2007).

Temperature conditions inside the spacecraft are maintained by protecting it from outer space extreme conditions e.g., charge particle bombardment through electrochemical coatings (Sheng 1996). The electrochemical coatings act as protecting layers or balancing temperature layers that are used on spacecraft. Keeping in view, the importance and need of thermal coatings, there must be some criteria for choosing thermal coatings and for materials that are used as a substrate for such thermal coatings. Aerospace industry has in general boosted the interest for materials having high strength to weight ratio (Joshi 2011). To get desired properties many researchers are doing efforts to design new alloys and to improve characteristics of existing alloys (Dixit 2008). The 7xxx series (Al-Zn-Mg-Cu alloy) have exceptional properties like high strength to density ratio (Puchi-Cabrera 2006), enhanced mechanical properties, high thermal and electrical conductivity, good resistance to oxidation and corrosion (Panigrahi 2011), improved wear resistance, high stiffness, low coefficient of thermal expansion (Ahamed 2011), recyclability and workability (Wu 1999). Due to these outstanding properties aluminum alloys are extensively used in development of aerospace structures (Roknia 2012). Replacement and repair of structural components of spacecrafts have significant issues so aluminum 7075 has utmost importance (Puchi-Cabrera 2006) to meet cost and weight requirements (Wu 1999). This high strength Al alloy has increased the life period of the structural parts of the space vehicles (Dasa 2011). But aluminum alloys cannot be used directly in space because of severe operating conditions.

Aluminum has pilling – Bedworth ratio (P- B ratio) > 1, due to which protective oxide layer is formed in air that provides protection against further surface oxidation (Bartolome 2008). This oxide layer is heterogeneous (Snogan 2002) and thin and its surface properties can be improved through electrochemical coatings (Cirik 2008).

Good thermal coatings are the one which has low solar absorptance and high infrared emittance values (Kumar 1999). The significance of infrared emittance is that, it controls the rate at which spacecraft emits radiations. The significance of solar absorptance for spacecraft is due to absorbed solar radiations that is the major external heat input to the spacecraft (Sharma 1997). Research has shown that combined effect of above natural and artificial factors, responsible for temperature anomalies in thermal status of the spacecraft also produces degradation in optical properties of the coatings (Blue 1992, Dury 2007). It causes solar absorptance factor to increase (Tonon 2001) that can jeopardize flight worthiness of the spacecraft (Ginell 1970). Therefore the role of optical properties is critical to maintain thermal control of the whole system and cannot be ignored for optimum performance of spacecraft (Anon 1997).

The severity of the impact of space environment on materials and coatings can be minimized by controlling the equilibrium temperature of the spacecraft by solar absorptance (αs) and infrared emittance (ε) (Babel 1996, Jayaraj 2004, Xiaohng 2008). In this research paper we have prepared alumina by sol-gel method. Sol-gel technique is low cost, simple and has numerous advantages as compare to any other technique.

Prepared samples were characterized by different tools for the investigation of properties.

2. EXPERIMENTAL DETAILS

Al_2O_3 was prepared by mixing two solutions A and B. Solution A was prepared by using $Al_2(SO_4)_3$ in 50 ml DI water with concentration 0.05 M. Solution B was prepared by using NaOH in 100 ml DI water with concentration 0.1 M. 50 ml of DI water was taken in a beaker and heated to 70°C.The two solutions were added drop wise by using two separate pipettes. After addition the precipitates were aged at 70°C for 3 h. Precipitates were centrifuged at 10,000 rpms for 1 min and then washed with DI water, ethanol and acetone. Finally, precipitates were dried at room temperature. Eight different samples were prepared by varying the ratio of $Al_2(SO_4)_3$ and NaOH the details of which are mentioned in Table 1.

A dispersion of precipitates was made by taking 5 ml DI water in beaker and precipitates were added and stirred for 20 min. Samples were then placed for ultrasonication for 20 min. Finally a milky dispersion was obtained (Viguie 2007).

To make thin films glass slides were cut with dimension 1 x 1 cm^2. Glass slides were washed with detergent. These washed slides were ultrasonically treated with acetone followed by isopropyl alcohol for 20 min each, and stored in isopropyl alcohol.

Thin films were deposited by the as prepared colloidal suspension of aluminum hydroxide made from above procedure having different ageing times. The spinning speed was adjusted at 3000 rpm for 15 seconds. After deposition the films were exposed to thermal treatment to obtain crystalline structure. Surface morphology was analyzed by Hitachi S-3400N Scanning electron microscopy while optical study was carried out with the help of J.A. Woollam Variable Angle Spectroscopic Ellipsometer (VASE).

Table 1 Ratio of $Al_2(SO_4)_3$/NaOH for preparation of Alumina nanoparticles

Sample	$Al_2(SO_4)_3$/NaOH ratio
S1	1:1
S2	1:2
S3	2:1
S4	1:3
S5	3:1
S6	1:4
S7	4:1
S8	1:5

3. RESULTS AND DISCUSSIONS

Surface morphology of Al_2O_3 thin films was observed by using SEM and Al_2O_3 micrographs has been shown in Figs. 1(a-h). Parida (2008) reported the formation of

Al_2O_3 nanostructure by precipitation method (Parida 2008). SEM micrograph of sample S1 aged at room temperature for 30 minutes, with thickness 199 nm has been shown in Fig. 1(a); micrograph shows the formation of thin film on the entire substrate. The average particle size came to be 90 nm. Fig. 1(b) shows the micrograph of Al_2O_3 aged at room temperature for 60 min sample named S2, thin film grown shows non uniformity of the film due to the presence of some larger particles with average particle size ~155 nm.

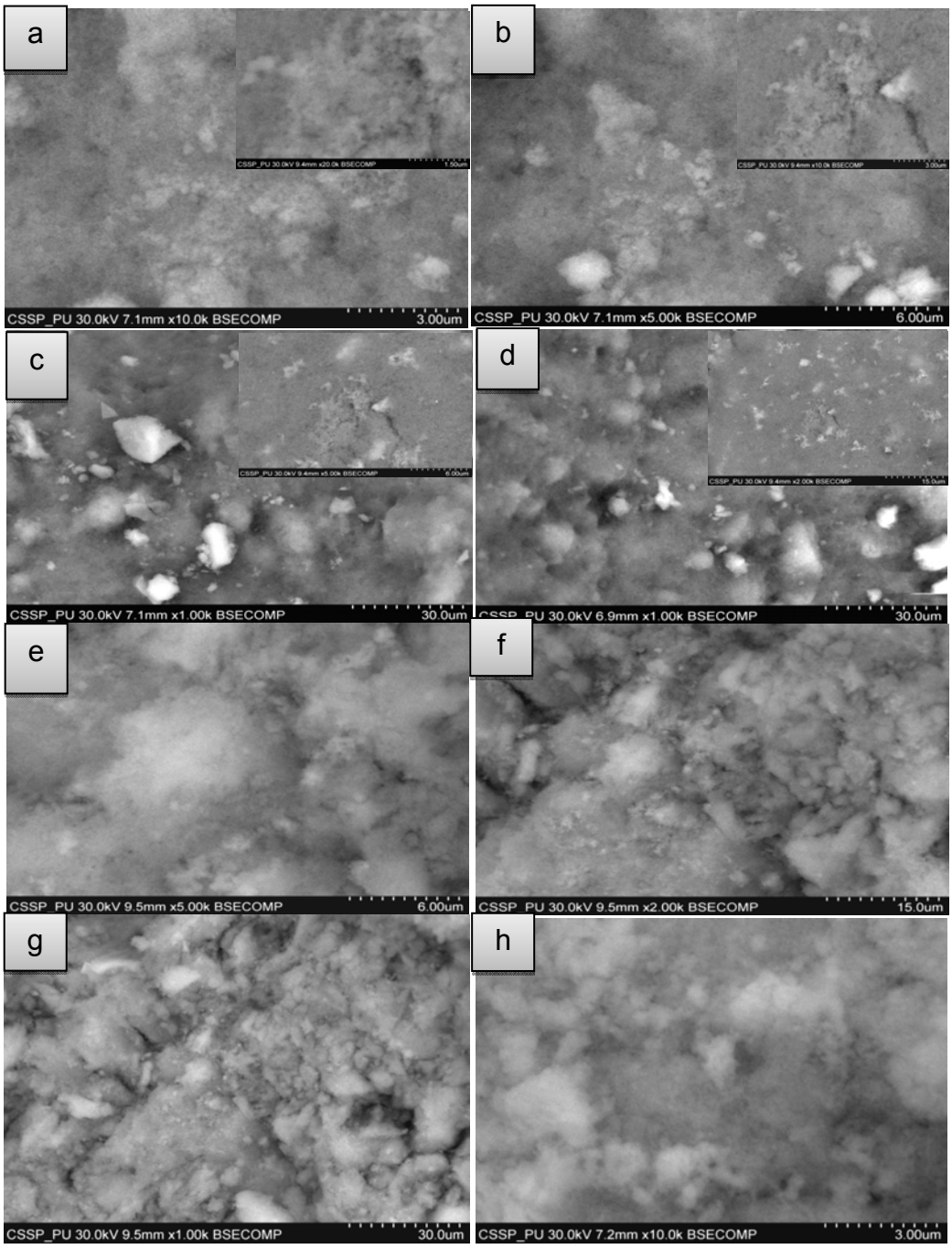

Fig. 1 SEM micrographs of alumina thin films

Al_2O_3 particles aged at 70°C for 30 minutes showed the formation of larger particles as compared to samples aged at room temperature. Fig. 1(c) is the micrograph of the sample S3 Al_2O_3 thin film and shows the presence of some larger particles resulting non uniformity of thin films. Average particle size is in the range of ~228 nm. Fig 1(d) is the micrograph of sample S4 aged 70°C for 60 min, and presents the interconnected structure and some wide pores and shows high density of particles with average particle size ~599 nm and thin film thickness i.e., 219 nm, resulting low transmission. Fig. 1(e) shows the micrograph of thin film sample S5 aged at 70°C for 60 min with 3 coatings and shows more dense structure when viewed at higher magnification, with average particle size of ~360 nm. Fig. 1(f) shows micrograph of thin film sample S6 aged at 70°C for 120 minutes, SEM micrograph shows larger pores and interconnected dense non-uniformly grown agglomerates of Al_2O_3 with average size of ~670 nm.

When Al_2O_3 particles were dispersed in water aggregates were formed on the expanse of smaller particles giving rise to large and dense particles throughout the sample. Fig. 1(g) is the micrograph of the thin film named S7 shows the presence of larger particles with average particle size ~1.46 μm, uniformly distributed causing less scattering and enhanced transmissions. Fig. 1(h) is the micrograph of thin film sample named S8 shows the agglomerates of larger dense Al_2O_3 particles dispersed in water, due to more number of coatings with film thickness of 211 nm with average particle size ~260 nm, a small decrease in transmission was observed.

Al_2O_3 thin films grown on glass substrates with different optimized conditions were analyzed by ellipsometery and their results are discussed as follows:

Fig. 2 shows the percentage of the optical transmission of Al_2O_3 thin films on glass substrate in wavelength range from 245 nm to 1500 nm. Al_2O_3 thin films show high transmission of light from visible to infrared region with average transmission for all

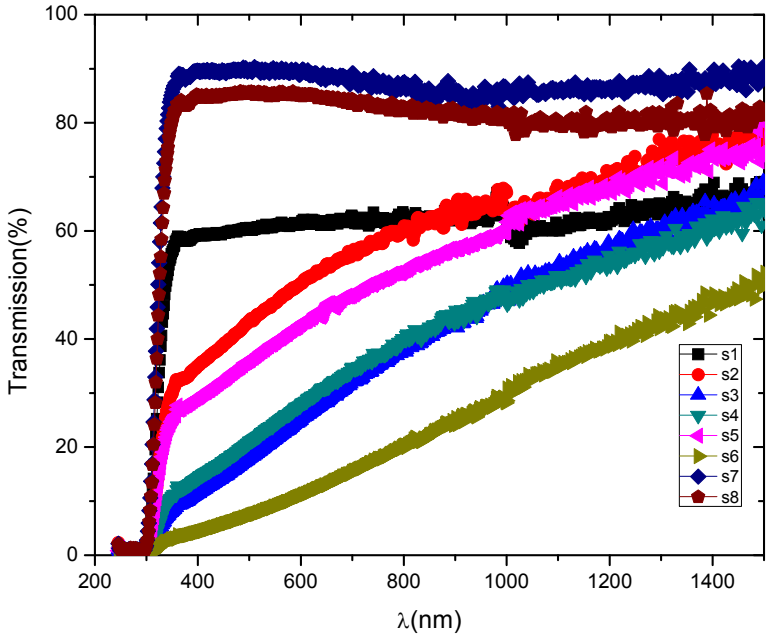

Fig. 2 Optical % transmission of Al_2O_3 thin films on glass substrate

the films greater than 52% as seen in Fig. 2. The sample S7 showed the maximum transmission of 91% in the visible region. With the increase of coating the film thickness increases from 199 nm to 219 nm. Tamboli et.al found the transmittance of Al_2O_3 thin films from 70% to 90% based on the film thickness and anions vacancies in the visible range (Tamboli 2011). As compared to the literature, the samples S7 and S8 showed the transmission of 89% and 84% respectively from visible to infrared portion of optical spectrum. Films S2, S3, S4, S5 and S6 show low values of transmission as compared to all other films. Decrease in transmission can be observed in the samples S2, S3, S4, S5 and S6 with the increase of aging time. This might be due to growth of grains and non-uniformity of thin films which ultimately results in the higher optical scattering.

A model fitting from the data obtained from experimental Spectroscopic Ellipsometery was used to obtain the refractive index and excitation coefficient k for the Al_2O_3 thin films. Al_2O_3 refractive index was observed from 1.4 to 1.7 in the wavelength range 300 nm to 500 nm as seen in Fig. 3. Value of n varies due to variation in the transmittance. Gündüz (2011), observed the refractive index in the range of 1.05 to 1.78 in the wavelength range of 200 nm to 800 nm, on the basis of film thickness by varying spin coating speed and annealing the films. Our peak values of refractive index are for sample S1 is 1.543 at wavelength 300 nm, 1.637 for S2 at 300 nm, 1.56 for S4

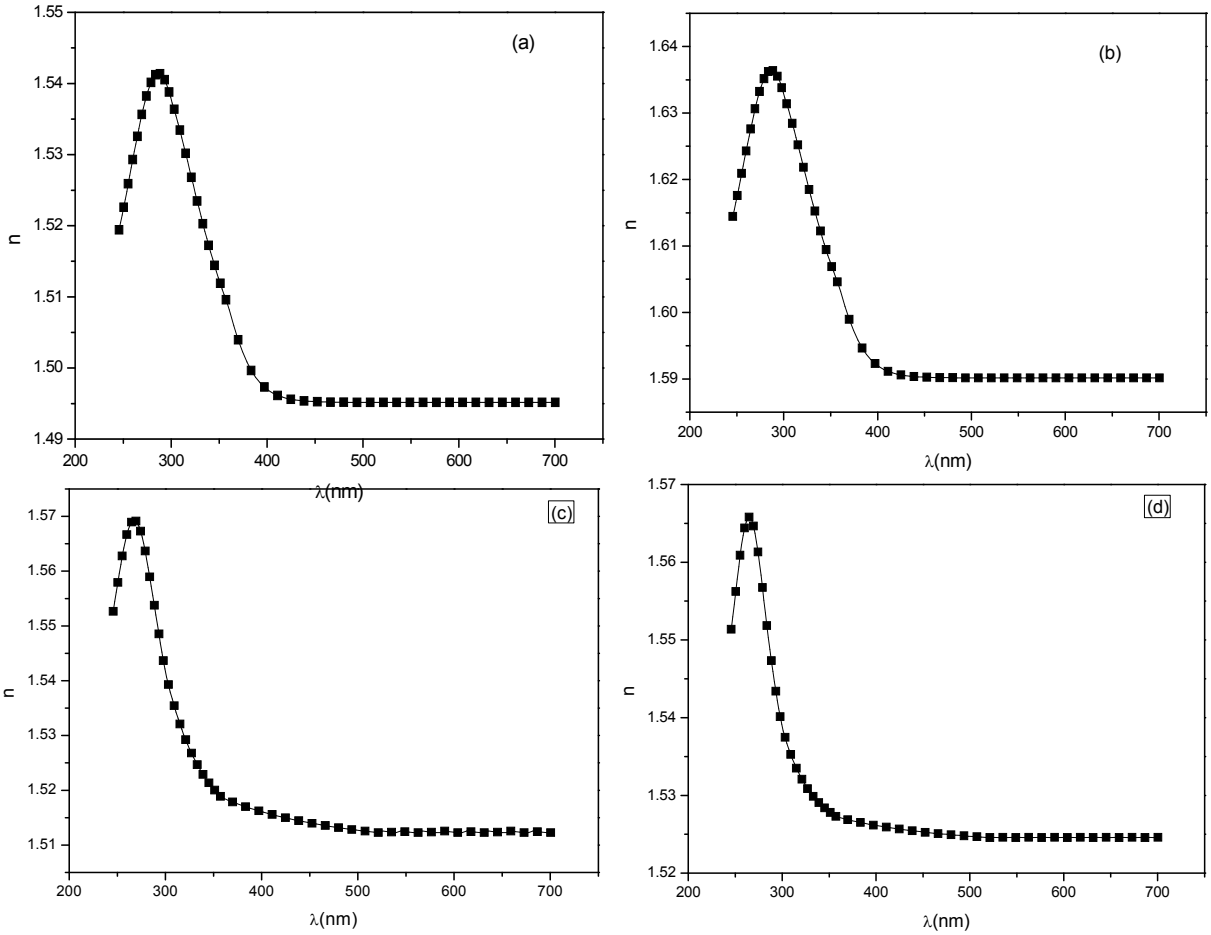

Fig. 3 Refractive index of Al_2O_3 thin films on glass substrate (a) S1; (b) S2; (c) S4; (d) S8

at 330 nm and 1.568 for S8 at 330 nm which is in good agreement with that reported in literature (Gündüz 2011).

Extinction coefficient of Al_2O_3 obtained from data has been shown in Fig. 4. The value of excitation coefficient of Al_2O_3 is in the range of 0.01 to 0.16 observed at wavelengths 300 nm to 500 nm. Extinction coefficient depends upon the absorption. Z.W. Zhao reported the extinction coefficient in the range from 0.01 to 0.05 for wavelength range 300 nm to 1200 nm for thin films prepared by off-plane filtered cathodic arc vacuum system with varied stichometry of oxygen anions (Zhou 2004). Fig. 4 shows extinction coefficient of Al_2O_3 thin films on glass substrate. We observed the peak values for extinction coefficient 0.103 for S1, 0.155 for S2, 0.064 for S4 and 0.083 for S8 all at 300 nm wavelength.

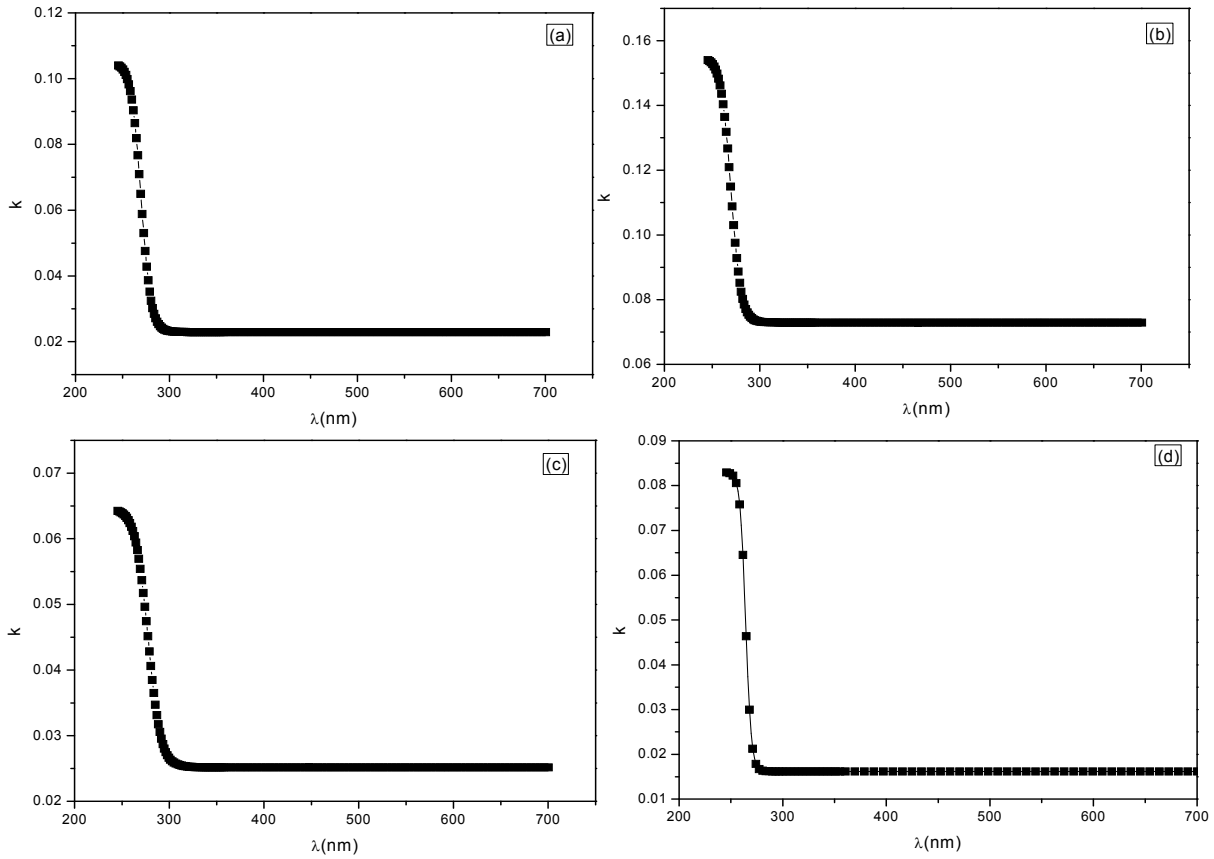

Fig. 4 Extinction coefficient of Al_2O_3 thin films on glass substrate (a) S1; (b) S2; (c) S4; (d) S8

Dielectric constant of thin films deposited on glass substrate was observed in the photon energy range of 2.0 eV to 5.0 eV. The data was taken at an angle of incidence of 45°. Cauchy model was used to fit experimental data in order to obtain the required optical properties i.e., refractive index and extinction coefficient. To calculate the dielectric constant we used Eq. (1).

$$\varepsilon = \varepsilon_1 + \iota\varepsilon_2 \tag{1}$$

Where ε_1 and ε_2 are real and imaginary dielectric constants and these real and imaginary parts of dielectric constant are calculated by using Eqs. (2) and (3).

$$\varepsilon_1 = n^2 - k^2 \tag{2}$$

$$\varepsilon_2 = 2nk \tag{3}$$

Gündüz (2011), found the dielectric constant of Al_2O_3 thin films grown by sol gel method by spin coating technique and optimized by varying the coating speed and annealing. Values of real part of dielectric constant were in the range of 1.0-3.0, and for imaginary part of dielectric constant was 0.01-0.60 in the energy region of 1 eV to 6 eV, varying with the thin film thickness and annealing. As compared to literature we observed peak values of dielectric constant as: for sample S1 real part of dielectric constant has value 2.38 at energy 4.3 eV and imaginary part of dielectric constant has value 0.32 at 5.0 eV. In case of sample S2 real part of dielectric constant has value of 2.67 at 4.3 eV and imaginary part has 0.5 at 5.0 eV. For sample S4 real part of dielectric constant has value of 2.46 at 4.3 eV and imaginary part has 0.2 at energy 5.0 eV. For sample S8 real part of dielectric constant has value of 2.45 at 4.5 eV and imaginary part of dielectric constant has value 0.253 at energy 5.0 eV. These variations might be due to the fact that thickness of these thin films varies resulting in the variation of the dielectric constant. Band gap of Al_2O_3 was obtained by finding the absorption coefficient of Al_2O_3, by using Eq. (4).

$$\alpha = \frac{1}{t}\ln\left[\frac{2R^2T}{-(1-R)^2 + \sqrt{(1-R)^4 + 4R^2T^2}}\right] \tag{4}$$

Here t is film thickness, T is transmission that is obtained from Spectroscopic Ellipsometer and R is reflection of the thin film. Band gap is measured at the absorption edge of the graph made by α^2 vs. energy. A graph was plotted between absorption and hu energy in the UV-Visible wavelength range. Value of band gap was observed by taking extrapolation of linear part on the energy axis.

Tamboli (2011) reported the band gap of Al_2O_3 thin films in the range of 4.5 eV to 5.8 eV for different thickness of the films in the range of 100 nm to 300 nm. In our case the band gap comes to be 3.96 eV for sample S1, 3.89 eV for sample S2, 3.77 eV for sample S4 and 3.97 eV for sample S8. Decrease of band gap as compared to bulk alumina may be due to the oxygen vacancies, or may be due to absorption defects or

Table 2 Optical properties of alumina thin films

Sample	Thickness (nm)	Refractive index (n)	Band gap (eV)
S1	199	1.540	3.96
S2	215	1.637	3.89
S4	219	1.560	3.77
S8	211	1.568	3.97

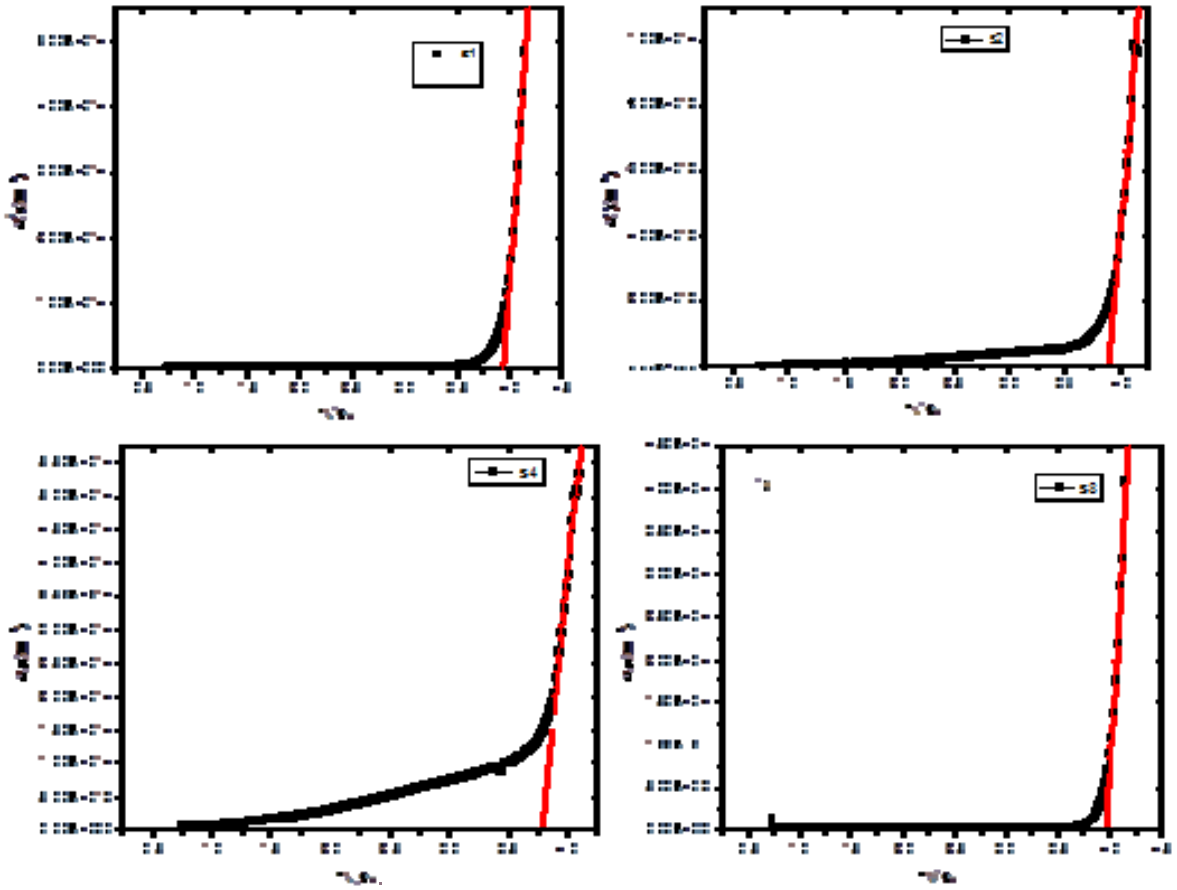

Fig. 5 Band gap of sample Al_2O_3 thin films on glass substrate of S1, S2, S4 and S8

due to amorphous nature of the films. Fig. 5 shows the band gaps of the three samples S1, S2, S4 and S8.

Table 2 represents the variation of band gap and refractive index with the variation of thin film thickness of Al_2O_3.

4. CONCLUSIONS

Aluminum oxide nanoparticles and alumina thin films were prepared by using sol-gel method by using different precursors. Aging temperature was varied from room temperature to 70°C to optimize the best conditions for the formation of nanoparticles and for uniform dense alumina films. Under optimized conditions, precipitates were centrifuged at 10,000rpms for 1 minute and then washed with DI water, ethanol and acetone and then thin films were grown by the as prepared colloidal suspension of aluminum hydroxide. The deposited alumina films were heat treated to get crystalline structure. SEM images have shown a change in grain size in the range of ~60- 90 nm after centrifugation. Grain size was observed to be strongly dependent on the choice of precursors, synthesis conditions and aging temperature. By increasing temperature and

time, particles tend to agglomerate resulted in larger size and non-uniformity. Energy band gap value was found to be ~4.13 eV. The refractive index was observed in the range of 1.55 to 1.79. Extinction coefficient value observed was ~ 0.103. Value of real and imaginary parts of dielectric constant was found to be ~ 2.83 and ~ 0.5, respectively.

REFERENCES

Ahamed, A., Neelay, A.J. and Shankar, K. (2011), "Experimental comparison of the effects of nanometric and micrometric particulates on the tensile properties and fracture behavior of Al composites at room and elevated temperatures", *Metall*. *Mater*. *Trans*. *A*, **42A**, 795-815.

Anon (1997), *Handbook of optical properties of thermal control surfaces*, Lockheed Missiles & Space Co.

Babel, H.W., Jones, C. and David, K. (1996), "Design properties for state-of -the-art thermal control materials for manned space vehicles in LEO", *Acta Astron*., **39**, 369-379.

Bartolome, M.J., Rio, J.F., Escudero, E., Feliu, S., Lopez, V., Otero, E. and Gonzalez, J.A. (2008), "Behaviour of different bare and anodised aluminum alloys in the atmosphere", *Surf*. *Coat*. *Technol*., **202**, 2783-2793.

Bensalah, W., Feki, M., Wery, M. and Ayedi, H.F. (2011), "Chemical dissolution resistance of anodic oxide layers formed on aluminum", *T*. *Nonferr*. *Met*. *Soc*., **21**, 1773-1679.

Blue, M.D. and Perkowitz, S. (1992), "Space-exposure effects on optical-baffle coatings at far-infrared wavelengths", *Appl*. *Opt*., **31**, 4305-4309.

Cirik, E. and Genel, K. (2008), "Effect of anodic oxidation on fatigue performance of 7075-T6 alloy", *Surf*. *Coat*. *Technol*., **202**, 5190-5201.

Dasa, P., Jayaganthan, R., Chowdhuryc, T. and Singh, I.V. (2011), "Fatigue behaviour and crack growth rate of cryorolled Al 7075 alloy", *Mater*. *Sci*. *Eng*. *A*, **528**, 7124-7132.

Dixit, M., Mishra, R.S. and Sankaran, K.K. (2008), "Structure–property correlations in Al 7050 and Al 7055 high-strength aluminum alloys", *J*. *Mater*. *Sci*. *Eng*. *A*, **478**, 163-172.

Dury, M.R., Thaeocharous, T., Harrison, N., Fox N. and Hilton, M. (2007), "Common black coatings-reflectance and aging characteristics in the 0.32-14.3 μm wavelength range", *Opt*. *Commun*., **270**, 262-272.

Fayazbakhsh, K. and Abedian, A. (2010), "Materials selection for applications in space environment", *Adv*. *Space Res*., **45**, 741-749.

Ginell, H. S. (1970). Nuclear and space radiation effects on materials. USA: National Aeronautics and space administration.

Goueffeon, Y., Aldebert, G., Mabru, C., Arurault, L., Tonon, C. and Guigue, P. (2009), "Study of degradation mechanisms of black anodic films in simulated space environment", *The 11th International Symposium on Materials in Space Environment*, Aix-en-Provence, France, 15-18.

Goueffeon, Y., Aldebert, G., Mabru, C., Arurault, L., Tonon, C. and Guigue, P. (2011),

"Flaking of black anodic films in space environment: Ageing and numerical simulation", *Mech*. *Mat*., **45**, 72-82.
Goueffeon, Y., Aldebert, G., Mabru, C., Arurault, L., Tonon, C. and Guigue, P. (2009), "Black anodic coatings for space applications: Study of the process parameters, characteristics and mechanical properties", *J*. *Mater*. *Process*. *Technol*., **209**, 5145-5151.
Gündüz, B., Cavaş, M. and Yakuphanoğlu, F. (2011), "Quality controlling of SiO_2 thin films by Sol Gel method", *The 6th International Advanced Technologies Symposium*, **6**, 569-573.
Hakimizad, A., Raeissi, K. and Ashrafizadeh, F. (2012), "Characterization of aluminum anodized layers modified in sulfuric and phosphoric acid baths and their effect on conventional electrolytic coloring", *Surf*. *Coat*. *Technol*., **206**, 2438-2445.
Jayaraj, B., Vishawiswaraiah, S., Desai, V.H. and Sohn, Y.H. (2004), "Electrochemical impedance spectroscopy of thermal barrier coatings as a function of isothermal and cyclic thermal exposure", *Surf*. *Coat*.*Technol*., **177-178**,140-151.
Joshi, S., Fahrenholtz, W.G. and O'Keefe, M.J. (2011), "Effect of alkaline cleaning and activation on aluminum alloy 7075-T6", *Appl*. *Surf*. *Sci*., **257**, 1859-1863.
Kumar, C.S., Mayanna, S.M., Mahendra, K.N., Sharma, A.K. and Rani, R. (1999), "Studies on white anodizing on aluminum alloy for space applications", *Appl*. *Surf*. *Sci*., **151**,280-286.
Kumar, C.S., Sharma, A.K., Mahendra, K.N. and Mayanna, S.M. (2000), "Studies on anodic oxide coating with low absorptance and high emittance on Aluminum alloy 2024", *Sol*. *Energy Mater*. *Sol*. *Cells*, **60**, 51-57.
Panigrahi, S.K. and Jayaganthan, R. (2011), "Effect of ageing on microstructure and mechanical properties of bulk, cryorolled and room temperature rolled Al 7075 alloy", *J*. *Alloys Compd*., **509**, 9609-9616.
Parida, K.M., Pradhan, A.C., Das, J. and Sahu, N. (2009), "Synthesis and characterization of nano-sized porous gamma-alumina by control precipitation method", *Mater*. *Chem*. *Phys*., **113**, 244-248.
Puchi-Cabrera, E.S., Gutie, C.V., Irausqu, I., Sosa, J.L.B. and Mesmacque, G. (2006), "Fatigue behavior of a 7075-T6 aluminum alloy coated with an electroless Ni–P deposit", *Int*. *J*. *Fatigue*, **28**, 1854-1866.
Qin, W., Cui, B., Wu, X.H. and Jiang, Z.H. (2007), "White anodic coatings on Aluminum alloy with low ratio of solar absorptance to infrared emittance", *Key Eng*. *Mater*., **336-338**, 643-646.
Riaz, S., Shamaila, S., Khan, B. and Naseem, S. (2008), "Lower temperature formation of alumina thin films through sol-gel route", *Surf*. *Rev*. *Lett*., **15**, 681.
Tamboli, S.H., Puri, V., Puri, R.K., Patil, R.B. and Luo, M.F. (2011), "Comparative study of physical properties of vapor chopped and nonchopped Al_2O_3 thin films", *Mater*. *Res*. *Bull*., **46**, 815-819.
Roknia, M.R., Hanzakia, A.Z. and Abedi, H.R. (2012), "Microstructure evolution and mechanical properties of back extruded 7075 aluminum alloy at elevated temperatures", *Mater*. *Sci*. *Eng*. *A*, **532**, 593-600.
Sharma, A.K., Bhojraj, H., Kaila, V.K. and Narayanamurthy, H. (1997), "Anodizing and inorganic black coloring of Aluminum alloys for space applications", *Met*. *Finishing*, **95**, 14-20.

Sheng, X.Y., Klampfl, B.F. and Barrera, E.V. (1996), “Effects of vacuum and vacuum-ultraviolet radiation on sulfuric acid anodized aluminum oxide coatings” *Scripta Mater*., **35**, 205-210.

Snogan, F., Blance, C., Mankowski, G. and Pebere, N. (2002), “Characterization of sealed anodic films on 7050 T-74 and 2214-T6 Aluminum alloys”, *Surf*. *Coat*. *Technol*., **154**, 94-103.

Tonon, C., Duvignacq, C.,Teyssedre, G. and Dinguirard, M. (2001), “Degradation of the optical properties of ZnO-based thermal control coatings in simulated space environment”, *J*. *Phys*. *D: Appl*. *Phys*., **34**,124-130.

Viguie, J.R., Sukmanowski, J., Nolting, B. and Royer, F.X. (2007), “Study of agglomeration of alumina nanoparticles by atomic force microscopy (AFM) and photon correlation spectroscopy (PCS)”, *Colloids and Surfaces A: Physicochem*. *Eng*. *Aspects*, **302**, 269-275.

Wu, Y.L., Froes, F.H., Li, C. and Alvarez, A. (1999), “Microalloying of Sc, Ni, and Ce in an advanced Al-Zn-Mg-Cu alloy”, *Metall*. *Mater*. *Trans*. *A*, **30A**, 1017-1024.

Xiaohng, W., Wei, Q., Bo, C., Zhaohua, J., Weiqiang, L. and Weidoung, H. (2008), “White anodized thermal control coating on LY12 Aluminum alloy”, *J*. *Mater*. *Process*. *Technol*., **200**, 405-409.

Yu, M., Jiang, W., Liu, J.H. and Li, S.M. (2011), “Black anodized thermal control coating on LY12 Aluminum alloy”, *Adv*. *Mater*. *Res*., **233-235**, 2166-2171.

Zhao, Z.W., Tay, B.K., Yu, G.Q., Chua, D.H.C., Lau, S.P. and Cheah L.K. (2004), “Optical properties of aluminum oxide thin films prepared at room temperature by off-plane filtered cathodic vacuum arc system”, *Thin Solid Films*, **14**, 447-448.